

Contents lists available at ScienceDirect

European Journal of Pharmaceutics and Biopharmaceutics

journal homepage: www.elsevier.com/locate/ejpb

Research paper

Biopharmaceutical profile of pranoprofen-loaded PLGA nanoparticles containing hydrogels for ocular administration

Guadalupe Abrego^{a,b}, Helen Alvarado^{a,b}, Eliana B. Souto^{c,d,*}, Bessy Guevara^b, Lyda Halbaut Bellowa^e, Alexander Parra^{a,b}, Ana Calpena^b, María Luisa Garcia^{a,*}

^a Department of Physical Chemistry, Faculty of Pharmacy, University of Barcelona, Barcelona, Spain^b Department of Biopharmacy and Pharmaceutical Technology, Faculty of Pharmacy, University of Barcelona, Barcelona, Spain^c Department of Pharmaceutical Technology, Faculty of Pharmacy, University of Coimbra (FFUC), Pólo das Ciências da Saúde, Coimbra, Portugal^d Center for Neuroscience and Cell Biology & Institute for Biomedical Imaging and Life Sciences (CNC-IBILI), University of Coimbra, Pólo das Ciências da Saúde, Coimbra, Portugal^e Department of Pharmacy and Pharmaceutical Technology, Faculty of Pharmacy, University of Barcelona, Barcelona, Spain

ARTICLE INFO

Article history:

Received 24 November 2014

Accepted in revised form 28 January 2015

Available online xxxxx

Chemical compounds:

Pranoprofen (PubChem CID:4888)

Keywords:

Pranoprofen

Nanoparticles

Hydrogel

Ocular tolerance

Physical stability

Corneal permeation

Anti-inflammatory efficacy

Azone

Non-steroidal anti-inflammatory drug

ABSTRACT

Two optimized pranoprofen-loaded poly-L-lactic-co glycolic acid (PLGA) nanoparticles (PF-F1NPs; PF-F2NPs) have been developed and further dispersed into hydrogels for the production of semi-solid formulations intended for ocular administration. The optimized PF-NP suspensions were dispersed in freshly prepared carbomer hydrogels (HG_PF-F1NPs and HG_PF-F2NPs) or in hydrogels containing 1% azone (HG_PF-F1NPs-Azone and HG_PF-F2NPs-Azone) in order to improve the ocular biopharmaceutical profile of the selected non-steroidal anti-inflammatory drug (NSAID), by prolonging the contact of the pranoprofen with the eye, increasing the drug retention in the organ and enhancing its anti-inflammatory and analgesic efficiency. Carbomer 934 has been selected as gel-forming polymer. The hydrogel formulations with or without azone showed a non-Newtonian behavior and adequate physicochemical properties for ocular instillation. The release study of pranoprofen from the semi-solid formulations exhibited a sustained release behavior. The results obtained from *ex vivo* corneal permeation and *in vivo* anti-inflammatory efficacy studies suggest that the ocular application of the hydrogels containing azone was more effective over the azone-free formulations in the treatment of edema on the ocular surface. No signs of ocular irritancy have been detected for the produced hydrogels.

© 2015 Elsevier B.V. All rights reserved.

1. Introduction

Pranoprofen is a non-steroidal anti-inflammatory drug (NSAID) which can be used as a safe and effective alternative anti-inflammatory treatment following strabismus and cataract surgery [1–3]. This drug has the beneficial effect of reducing the ocular signs and symptoms of dry eye and decreasing the inflammatory markers of conjunctival epithelial cells [4]. Its efficacy is equivalent to moderate-potency corticosteroids, but it has improved safety profile. It should be considered for the treatment of chronic conjunctivitis of presumed nonbacterial origin [5]. Although this drug has shown high anti-inflammatory and analgesic efficiency, the pharmaceutical use of pranoprofen is limited due to its inadequate biopharmaceutical profile. Pranoprofen has a short plasmatic half-life, low water solubility and is unstable in aqueous solution, particularly when exposed to light [6,7]. Pranoprofen is commercially available as eye-drops (0.1% m/V). However, this conventional dos-

Abbreviations: PF, pranoprofen; NPs, nanoparticles; HG, hydrogel; PF-F1NPs and PF-F2NPs, optimized pranoprofen nanoparticles; HG_PF-NPs-Azone and HG_PF-NPs, nanoparticles incorporated into hydrogel with and without azone, respectively; Z-Ave, average particle size; PI, polydispersity index; ZP, zeta potential; EE, entrapment efficiency; PVA, polyvinyl alcohol; cPF, PF concentration; cPVA, PVA concentration; PLGA, poly-L-lactic-co glycolic acid; cPLGA, PLGA concentration; SA, arachidonic acid sodium; PBS, phosphate buffer solution; BR, Bicarbonate Ringer; Q_p , amounts of drug permeated across cornea; Q_r , amounts of drug retained in the cornea.

* Corresponding authors. Department of Pharmaceutical Technology, Faculty of Pharmacy, University of Coimbra (FFUC), Pólo das Ciências da Saúde, Azinhaga de Santa Comba, 3000-548 Coimbra, Portugal. Tel.: +351 239 488 400; fax: +351 239 488 503 (E.B. Souto). Department of Physical Chemistry, Faculty of Pharmacy, University of Barcelona, Av. Joan XXIII s/n, 08028 Barcelona, Spain. Tel.: +34 934 021 220; fax: +34 934 021 231 (M.L. Garcia).

E-mail addresses: esouto@ff.uc.pt (E.B. Souto), marisagarcia@ub.edu (M.L. Garcia).

<http://dx.doi.org/10.1016/j.ejpb.2015.01.026>

0939-6411/© 2015 Elsevier B.V. All rights reserved.

age form cannot be considered optimal in the treatment of ocular diseases due to the fact that upon instillation most of the drugs are removed from the surface of the eye, by various mechanisms (tear dilution and tear turn over). Moreover, the relatively impermeable corneal barrier restricts the entry of foreign substances. As a result, less than 5% of the administered drug penetrates the cornea and reaches intraocular tissue [8]. Polymeric NPs are one of the colloidal systems that have been most widely studied over the past few decades with the objective of improving drug targeting of tissues and organs and increase drug bioavailability across biological membranes. Biodegradable polymers, such as poly (lactic-co-glycolic) acid (PLGA), have been widely used in drug delivery research, in part due to their approval by the FDA for use in humans and they can effectively deliver the drug to a target site with a controllable degradation [9]. PLGA can be used such as matrix to load different drugs for topical administration [10–12].

Different drug delivery systems have been studied in order to improve drug targeting of tissues, increase drug bioavailability across biological membranes or reducing its toxicity. For topical application of nanoparticle suspensions, several of these systems have been dispersed in semi-solid vehicles such as hydrogels or cream [13,14]. Among the gelling agents, carbomer has been extensively used for design topical formulations [15–17]. In addition, to improve the permeability of drugs through the ocular barriers, different enhancers have also been tested. Azone is one of the most widely studied penetration enhancers which can be used as a safe and effective penetration enhancer for human use in the range of 1–10% [18]. In previous studies, we have formulated pranopfen in PLGA nanoparticles (PF-NPs) using the solvent displacement technique [19]. A 2⁴ central composite factorial design has been applied to study the main effects and interactions of four factors on average particle size (Z-Ave), polydispersity index (PI), zeta potential (ZP) and entrapment efficiency (EE). The factors studied were PF concentration (cPF), PVA concentration (cPVA), PLGA concentration (cPLGA) and aqueous phase pH. From a total of 26 formulations obtained by factorial design, two optimum formulations (PF-F1NPs and PF-F2NPs) were selected for further investigation here [20]. The aim of this study was designed semi-solid formulations containing pranopfen loaded-PLGA nanoparticles for ocular administration. Carbomer 934 was selected to disperse the optimized PF-NP suspension because of the bioadhesive properties, low or no toxicity, rheological characteristics and biocompatibility of the hydrophilic polymer. Polyacrylic acid hydrogels such as Carbomer 934, polycarbophil and carboxymethylcellulose have been reported as the most appropriate bioadhesive polymers for ocular drug delivery [21]. Additionally, the high viscosity of the carbomer hydrogels ensures the prolonged retention improving the ocular bioavailability of some drugs [22]. The optimized PF-F1NP and PF-F2NP suspensions were dispersed into blank hydrogels (HG_PF-F1NPs and HG_PF-F2NPs) or in hydrogels containing 1% azone (HG_PF-F1NPs-Azone and HG_PF-F2NPs-Azone) in order to improve the biopharmaceutical profile of pranopfen in the eye, by increasing its ocular retention and improving the anti-inflammatory and analgesic efficiency. The ultimate aim of the developed formulations is to improve the patient's compliance to the pharmacological treatment by reducing the application frequency. In this study, azone was selected as permeation enhancer with the purpose to improve the permeability of pranopfen from PF-NPs based HG through the ocular barriers. Azone is one of the most widely studied penetration enhancers for hydrophilic and lipophilic drugs. As a penetration enhancer, azone is more effective at low percentages (1–3%), and it has also been reported to be of low irritancy and very low toxicity [23]. The mechanism of azone may be related to some changes in the epithelial cell junctions of the cornea, which are nevertheless reversible in cornea structure [24,25].

The physicochemical properties and the rheological behavior of HG_PF-NP formulations have been characterized. The physical stability of the nanoparticles incorporated into hydrogels has also been evaluated. *In vitro* release profile and *ex vivo* corneal permeation of pranopfen from the semi-solid formulations, as well as their *in vitro* e *in vivo* ocular tolerance and the anti-inflammatory efficacy have also been assayed.

2. Materials and methods

2.1. Materials

Pranopfen and Oftalar[®] were kindly supplied by Alcon Cusi (Barcelona, Spain); PLGA Resomer[®] 753S was obtained from Boehringer Ingelheim (Ingelheim, Germany). Polyvinyl alcohol (PVA) with 90% hydrolyzation and Arachidonic acid sodium (SA) were obtained from Sigma Aldrich (St. Louis, USA). Gel-forming polymer (Carbomer 934) was obtained from Fagron Ibérica. The purified water used in all the experiments was obtained from a MilliQ System. All the other chemicals and reagents used in the study were of analytical grade.

2.2. Methods

2.2.1. Preparation of pranopfen-loaded nanoparticles

The nanoparticles have been produced by the solvent displacement technique, described by Fessi et al. [19]. PLGA (90 mg or 95 mg) and pranopfen (10 mg or 15 mg) were dissolved in 5 mL of acetone. This organic phase was poured, under moderate stirring into 10 mL of an aqueous solution of PVA (5 mg/mL or 10 mg/mL) adjusted to the desired pH value (4.5 or 5.5). The acetone was then evaporated and the dispersed nanoparticles were concentrated to 10 mL under reduced pressure (Büchi B-480 Flawil, Switzerland). Table 1 shows the composition of the optimized pranopfen-loaded nanoparticles.

2.2.2. Mean particle size and zeta potential

The mean particle size (Z-Ave) and the zeta potential (ZP) of the nanoparticles were determined by photon correlation spectroscopy (PCS) with a Zetasizer Nano ZS (Malvern Instruments, Malvern, UK) at 25 °C using disposable quartz cells and disposable folded capillary zeta cells (Malvern Instruments, Malvern, UK), respectively. For all measurements, the samples were diluted with MilliQ water (1:20). The reported values are the mean ± SD of at least three different batches of each formulation.

2.2.3. Encapsulation efficiency

The encapsulation efficiency (EE) of pranopfen in the nanoparticles was determined indirectly by measuring the concentration of the free drug in the dispersion medium. The non-encapsulated pranopfen was separated using a filtration/centrifugation technique with Ultracel-100K (Amicon[®] Ultra, Millipore Corporation, Billerica, MA) centrifugal filter devices at 3000 rpm for 30 min at 4 °C (Heraeus, Multifuge 3 L-R, centrifuge, Osterode, Germany). Each sample was diluted with MilliQ water (1:20) prior to filtration/centrifugation. The EE was calculated using the following equation:

Table 1

Composition of the optimized pranopfen-loaded nanoparticles.

| PF-NPs | cPF (mg/mL) | cPVA (mg/mL) | cPLGA (mg/mL) | pH |
|----------|-------------|--------------|---------------|-----|
| PF-F1NPs | 1.5 | 10.0 | 9.5 | 5.5 |
| PF-F2NPs | 1.0 | 5.0 | 9.0 | 4.5 |

$$EE(\%) = \frac{\text{Total Amount of pranoprofen} - \text{Free drug}}{\text{Total Amount of pranoprofen}} \times 100 \quad (1)$$

The assay was carried out by high performance liquid chromatography (HPLC) using a method previously validated in our laboratory. The detection and quantification limits (LOD and LOQ) found for the validated method were $1.05 \pm 0.70 \mu\text{g/mL}$ and $3.17 \pm 2.12 \mu\text{g/mL}$, respectively. The HPLC system consisted of a Waters 1525 pump (Waters, Milford, USA) with a UV-Vis 2487 detector (Waters), a flow rate of 1 mL/min and wavelength of 245 nm were used with a (Kromasil[®], 100-5C18, $4.6 \times 100 \text{ mm}$) column. The mobile phase consisted of methanol: glacial acetic acid 5% (45: 55, v: v).

2.3. Preparation of pranoprofen-loaded nanoparticles dispersed in hydrogels

The blank hydrogels were prepared with carbomer (1% w/v), dispersed in purified water and allowed to hydrate for 24 h. Subsequently, glycerol (3% w/w) and azone (0% or 1% w/w) were incorporated into the hydrogel by stirring for 5 min at 1000 rpm in a high speed stirred (Cito Unguator Konietzko, Bamberg, Germany) and then the pH was adjusted at 6.5 with 0.1 N NaOH. The HG was left to equilibrate for 24 h at room temperature before used. The optimized aqueous PF-NP suspensions were incorporated into HG with 0% or 1% azone using a high speed stirred by 3 min at 1000 rpm, in a concentration of 50% (w/w) of the nanoparticle dispersion into the hydrogel.

2.4. Physicochemical characterization of the hydrogels

The morphological examination of the NPs incorporated into HG was performed by Transmission Electron Microscopy (TEM). The sample was dispersed in MilliQ water using an Elma Transonic Digital S T490 DH ultrasonic bath (Elma, Singen, Germany). A drop of this dispersion (10 μL) was placed on copper electron microscopy grids and stained with a 2% (w/v) uranyl acetate solution. After 1 min, the sample was washed with ultra-purified water and the excess fluid removed with a piece of filter paper. The dried sample was then examined.

The physical stability of the HG_PF-NP formulations was assessed after 1 day of the production and 90 days of storage at 25 °C. The Z-Ave and ZP of the particles were determined by photon PCS as described above. The diameter of the nanoparticles dispersed into the hydrogels also was measured by laser diffraction (LD) data, obtained with a Mastersizer Hydro 2000MU (Malvern Instruments Ltd., Malvern, UK), using the volume distribution as diameter values of LD 10%, LD 50% and LD 90%. The diameter values indicate the percentage of nanoparticles showing a diameter equal or lower than the given value. For all measurements, the samples were dispersed in MilliQ water using an Elma Transonic Digital S T490 DH ultrasonic bath (Elma, Singen, Germany).

2.5. Rheological measurements of the hydrogels

The hydrogel samples were placed in glass vials with rubber top and aluminum capsule and storage at 25 °C \pm 2 °C. The rheological characterization of each formulation was performed using a Haake Rheostress1 rheometer (Thermo Fisher Scientific, Karlsruhe, Germany) connected to a temperature control Thermo Haake Phoenix II + Haake C25P and equipped with parallel plate geometry (Haake PP60 Ti, 60 mm diameter, 0.5 mm gap between plates) or cone plate set-up with a fixed lower plate and a mobile upper cone (Haake C35/2° Ti, 35 mm diameter, 0.106 mm gap between cone-plate). The viscosity curves and flow curves were recorded under rotational runs at 25 °C for 3 min during the ramp-up period

from 0 to 100 s^{-1} , 1 min at 100 s^{-1} (constant shear rate period) and finally 3 min during the ramp-down period from 100 to 0 s^{-1} . Viscosity values at 100 s^{-1} were determined after 8 days of the production and 90 days of storage at 25 \pm 2 °C, in three replicates. Oscillatory stress sweep tests were performed at a constant frequency of 1 Hz in a stress range of 0.1 and 200 Pa. Oscillation frequency tests were carried out from 0.01 to 10 Hz at a constant shear stress within the linear viscoelastic region, in order to determine the related variation of storage modulus (G') and loss modulus (G'') at 25 °C. The software Haake RheoWin[®] Job Manager V.3.3 and RheoWin[®] Data Manager V.3.3 (Thermo Electron Corporation, Karlsruhe, Germany) were used to carry out the test and analysis of the obtained data, respectively.

2.6. In vitro pranoprofen release from the hydrogels

In vitro release study of pranoprofen from the HG_PF-NP formulations was performed in Franz diffusion cells [26]. These cells consist of a donor and a receptor chamber between which a membrane is positioned. A dialysis membrane (MWCO 12,000–14,000 Da., Dialysis Tubing Visking, Medicell International Ltd., London, UK) was used. The membrane was hydrated for 24 h before being mounted in the Franz diffusion cell. The experiment was performed under “sink condition”. The HG_PF-NP formulations were compared with the commercial eye drops (Oftalar[®], pranoprofen 1 mg/mL) and the free drug (1 mg/mL) dissolved in phosphate buffer solution (PBS) at pH 7.4. A weight of 400 mg of the HG_PF-NP formulations or a volume of 200 μL of the free drug solution and commercial eye drops was placed in the donor compartment and the receptor compartment was filled with PBS at pH 7.4 kept at 37 \pm 0.5 °C. A volume of 300 μL was withdrawn from the receptor compartment at fixed times and replaced by an equivalent volume of fresh PBS at the same temperature. The concentration of pranoprofen released was measured as described previously for EE. Values are reported as the mean \pm SD of three replicates.

The amount pranoprofen release was adjusted to the following kinetic models [27]:

$$\text{Zero order : } \%R_t/\%R_\infty = k \times t \quad (2)$$

$$\text{First order : } \%R_t/\%R_\infty = 1 - e^{-k \times t} \quad (3)$$

$$\text{Higuchi : } \%R_t/\%R_\infty = k \times t^{1/2} \quad (4)$$

$$\text{Hyperbola : } \%R_t/\%R_\infty = R_\infty \times t/(k + t) \quad (5)$$

$$\text{Korsmeyer–Peppas : } \%R_t/\%R_\infty = k \times t^n \quad (6) \quad 288$$

where $\%R_t$ is the percentage of the drug released at time t , $\%R_\infty$ is the total percentage of drug released, $\%R_t/\%R_\infty$ is the fraction of drug released at time t , k is the release rate constant and n is the diffusion release exponent that can be used to characterize the different release mechanisms; $n \leq 0.5$ (Fickian diffusion), $0.5 < n < 1.0$ (anomalous transport), and $n \geq 1$ (case II transport, i.e., zero-order release). A nonlinear least-squares regression was performed using the WinNonLin[®] software (WinNonLin[®] professional edition version 3.3 and Graphpad prism version 6 Demo) and the model parameters were calculated. Akaike's information criterion (AIC) was determined for each model as an indicator of the model's suitability for a given dataset [28].

2.7. Corneal permeation study

Ex vivo corneal permeation experiments were carried out with New Zealand rabbits (male, weighing 2.5–3.0 kg), under veterinary supervision and according to the Ethics Committee of Animals Experimentation at the University of Barcelona. The rabbits were anesthetized with intramuscular administration of ketamine HCl (35 mg/kg) and xylazine (5 mg/kg). The animals were euthanized

by an overdose of sodium pentobarbital (100 mg/kg) administered through marginal ear vein under deep anesthesia. The corneas, with 2 mm ring of sclera were excised and immediately transported to the laboratory in artificial tear solution. The assay was done using Franz diffusion Cells. The cornea was fixed between the donor and receptor compartment of Franz cell. The corneal area available for permeation was 0.64 cm². The receptor compartment was filled with freshly prepared Bicarbonate Ringer's (BR) solution. This compartment was kept at 37 ± 0.5 °C and stirred continuously. A weight of 1 g of the HG_PF-NP formulations or 1 mL of the commercial eye drops and free drug solution was placed in the donor compartment (covered with parafilm[®] in order to avoid evaporation). A volume of 300 µL was withdrawn from the receptor compartment at fixed times and replaced by an equivalent volume of fresh BR solution at the same temperature. The cumulative pranoprofen amount permeated through the cornea per unit area (µg/cm²) was calculated, at each time point, from cPF in the receiving medium and plotted as function time (min).

2.8. Amount of pranoprofen retained in the cornea

At the end of the study, the cornea was used to determine the amount of drug retained. The cornea was carefully freed from the sclera ring, cleaned using a 0.05% solution of sodium lauryl sulfate and washed with distilled water, weighed and treated with methanol: water (50:50, V/V) under sonication during 30 min using an ultrasound bath. The amount of pranoprofen permeated and retained through the cornea was determined by HPLC as described previously for EE. The results are reported as the median ± SD and median value (minimum – maximum range) of six and three replicates for the amount of pranoprofen permeated and retained, respectively.

2.9. Ocular permeation parameter

Lag time T_L (h) values were calculated by plotting the cumulative pranoprofen permeating the cornea versus time, determining x-intercept by linear regression analysis. The corneal permeability coefficient K_p (cm/h), partition coefficient P_1 (cm) and diffusion coefficient P_2 (h⁻¹) were calculated from the following equations:

$$K_p = P_1 \times P_2 \quad (7)$$

$$P_1 = J/(A \times C_0 \times P_2) \quad (8)$$

$$P_2 = 1/(6 \times T_L) \quad (9)$$

where C_0 is the initial concentration of drug in the donor compartment, A (0.64 cm²) is the exposed corneal surface. All the values are reported as median value (minimum – maximum range) of three replicates. Experimental data were processed using Graphpad prism software (version 6 Demo) and compared by the application of a non-parametric statistical Kruskal–Wallis Z test followed by the Dunn's multiple comparison tests. Values were considered to be significant at $p < 0.05$.

2.10. Corneal hydration levels

The corneal hydration level HL (%) of the cornea was determined at the end of the study of corneal permeation. The cornea was carefully freed from the sclera ring, washed, weighed (W_w) and desiccated at constant weight dried at 80 °C and then reweighed (W_d). The HL values are reported as median value (minimum – maximum range) of three replicates. HL was calculated using the following expression:

$$HL = [1 - (W_d/W_w) \times 100] \quad (10)$$

2.11. In vitro ocular tolerance

The ocular tolerance of the HG_PF-NP formulations with a 0% or 1% azone was assessed by the HET-CAM test. This is an alternative to animal testing (Draize test) described by Luepke [29]. To perform it, the shell and the inner membranes of 10-day-old chicken eggs were previously removed, so that the CAM that separates the embryo from the air chamber was visible, according to the Invitox protocol [30], and the Journal officiel de la République Française [31]. Tolerance was assessed by testing 6 eggs for each sample, using 2 eggs treated with 0.1 N NaOH and 2 treated with 1% sodium lauryl sulfate solution as positive controls. After exposing the CAM and rinsing it with PBS at pH 7.4, 300 µL of the test solution was applied to the CAM. The intensity of the reaction was semi-quantitatively assessed on a scale from 0 (no reaction) to 3 (strong reaction). The time of the appearance and the intensity of any reactions that occurred within 5 min were recorded. The ocular irritation index (OII) was then calculated using the following equation:

$$OII = \frac{(301 - h) \times 5}{300} + \frac{(301 - l) \times 7}{300} + \frac{(301 - c) \times 9}{300} \quad (11)$$

where h is the time (in seconds) until the start of a hemorrhage, l until the start of lysis and c until the coagulation. The following classification was used: $OII \leq 0.9$: slightly irritating; $0.9 \leq OII \leq 4.9$: moderately irritating; $4.9 \leq OII \leq 8.9$: irritating; $8.9 \leq OII \leq 21$: severely irritating.

2.12. In vivo ocular tolerance

The irritancy of the HG_PF-NP formulations with a 0% or 1% azone was evaluated in New Zealand white rabbits (2.5–3.0 kg) following the method described by Draize et al. [32,33]. A single instillation of 50 µL of each HG_PF-NP formulation was instilled in one eye, using untreated contra-lateral eye as a control. Readings were performed 1 h after sample application, then after 1, 2, 3, 4 and 7 days. The method provided an overall scoring system for grading the severity of ocular lesions involving the cornea (opacity), iris (inflammation degree) and conjunctiva (congestion, swelling and discharge). The Draize score was determined by visual assessment of change in these ocular structures. The mean total score (MTS) was calculated as follows:

$$MTS = \frac{X_1(n)}{2} + \sum \frac{X_2(n)}{2} - \sum \frac{X_3(n)}{5} \quad (12)$$

where x_1 (n), x_2 (n) and x_3 (n) are the cornea, conjunctiva and iris scores, respectively, being n the number of rabbits included in the ocular tolerance assay.

2.13. In vivo anti-inflammatory efficacy

The anti-inflammatory efficacy of the HG_PF-NP formulations was assessed using the method described by Spampinato Santi et al. [34], the ocular inflammation was induced by ocular instillation of 50 µL SA (dissolved in PBS, 0.5% (w/v)) in the right eye of eight groups of six rabbits (including control group). A volume of 50 µL of each HG_PF-NP formulation or 0.9% (w/v) isotonic saline solution (control group) was instilled in the conjunctival sac of the right eye 30 min before induction of ocular inflammation by SA using left eye as an inflammation control. Inflammation was quantified 30 min after AS instillation, then after 60, 90, 120, and 150 min, according to a modified Draize scoring system [32]. The MTS was calculated as described previously in the ocular tolerance assay (Eq. (12)). Since corneal transparency was not affected by the instillation of SA, this parameter was not considered. The sum of the conjunctival and iris score is expressed by the mean ± SD.

3. Results and discussion

3.1. Physicochemical characterization of the HG_PF-NPs

In previous studies, we have formulated pranoprofen in PLGA nanoparticles as new delivery system suitable for the ocular route. The Z-Ave of the optimized PF-F1NP and PF-F2NP formulations was around 350 nm with PI values in the range of mono-disperse systems ($PI < 0.1$). Both formulations had net negative charge with ZP values of -7.41 mV and -8.5 mV for PF-F1NPs and PF-F2NPs, respectively. The percentage of encapsulated pranoprofen in the polymeric matrix for these formulations reached 80% [20]. For the present work, carbomer 934 was selected as hydrogel matrix to incorporate the optimized PF-F1NP and PF-F2NP suspensions in order to improve the biopharmaceutical profile of pranoprofen for the ocular application. The size and surface morphology of the optimized PF-NPs after incorporation into HG were determined by TEM. The mean diameters of HG_PF-NP formulations were around 300 nm.

TEM image depicted in Fig. 1 reveals that the optimized NPs after incorporation into HG were spherical shape and non-aggregated. The results obtained show that the Z-Ave of the NPs incorporated into HG was similar to those of the NP suspensions.

The stability of the nanoparticles dispersed into the hydrogels was assessed after 1 day of the production and after 90 days of storage at 25 °C. The results obtained by DL 1 day after the production reveal two peaks, one at about 400 nm and another small peak at 1 μm for all the HG_PF-NP formulations indicating an increase of the Z-Ave and PI of the PF-NPs after incorporated into the hydrogels (see Fig. a, c, e and g in Supplementary materials). After 90 days of storage at 25 °C, an increase in the Z-Ave values compared with the results obtained 1 day after the production (see Fig. b, d, f and h in Supplementary materials). The results given in Table 2 show that the Z-Ave values obtained by PCS were similar to those obtained by DL. This increase in the apparent particle size was attributed to the strong entrapment of the particles within the

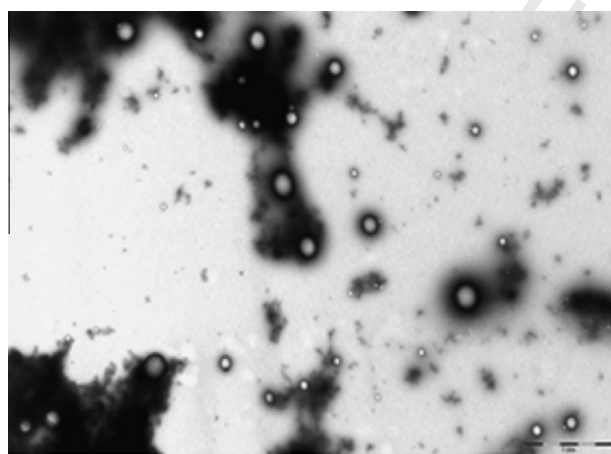


Fig. 1. Transmission electron microphotograph of the optimized NPs incorporated into hydrogel.

tridimensional gel structure, rather than real particle agglomerates. These results are in accordance with those obtained by Gonzalez-Mira et al. [35]. These results are also in agreement with those obtained by TEM (Fig. 1), since PF-NPs incorporated into HG showed similar particle size in comparison with PF-NP suspension and they were not aggregated. The particle size of formulations intended for ocular instillation is of crucial importance and it should not exceed 10 μm; larger sizes may cause a scratching feeling of a foreign body in the eye and it would therefore compromise patient's comfort [36,37]. The results obtained by PCS in Table 2 also revealed a significant increase of the ZP values of the PF-NPs after incorporated into hydrogels. These results were attributed to the adsorption of negatively charge of the jellifying agent molecules onto the surface of the particles [38]. All the results obtained from the stability study show that the HG_PF-NPs with or without azone formulations exhibit appropriate physicochemical properties for ocular administration, which indicates that the gel network of carbomer could not influence the morphology and size of the NPs notably.

3.2. Rheological measurements

The results obtained from the rheological characterization of the HG_PF-NP formulations with or without azone are shown in Table 3.

The rheological characterization of the HG_PF-NP formulations with or without azone revealed a non-Newtonian behavior and the pseudo-plastic character. The spreading properties and the ability of controlling their viscosity showed for the HG_PF-NPs are desirable for the ocular application. The results obtained in Table 3 show that the HG_PF-NP formulations after 90 days of storage at 25 °C exhibited a decreased of the viscosity and Thixotropy values regarding to the values observed at 8 days of the production. Table 3 also reveals that the inclusion of azone in the HG_PF-NP formulations leads a significant viscosity increase in the HG_PF-F1NPs-Azone and HG_PF-F2NPs-Azone formulations. These results are in accordance with the increase of the Z-Ave and PI obtained after 90 days of storage at 25 °C obtained by LD (see Figure in Supplementary material) and PCS (Table 2) which could be explained by the fact that the NPs characterized by a wide polydispersity could pack better than those with a narrow polydispersity. The particles with a large polydispersity have more free space to move around, which means that it was easier for the sample to flow and a lower viscosity would be measured [39].

The oscillation frequency test was carried out from 0.01 to 10 Hz at a constant shear stress within the linear viscoelastic region, in order to determine the related variation of storage modulus (G') and loss modulus (G'') at 25 °C, where the G' describes the elastic properties whereas G'' describes the viscous properties of the sample.

With respect to the stress sweep test of the oscillatory study, the critical stress was found at 10 Pa for the semi-solid formulations assayed. These results suggest that none of the formulations showed a weak structure. From the results of oscillatory stress sweeps, a constant shear stress of 2 Pa (20% of the critical value) was selected to perform the frequency sweep tests. The oscillatory measurements applied to the formulations showed the prevalence

Table 2

Mean particle size (Z-Ave) and zeta potential (ZP) of the HG_PF-NP formulations 1 day after production and after 90 days of storage at 25 °C.

| Time Day | HG_PF-F1NPs | | HG_PF-F2NPs | | HG_PF-F1NPs-Azone | | HG_PF-F2NPs-Azone | |
|-------------|---------------|---------------|---------------|---------------|-------------------|---------------|-------------------|---------------|
| | Z-Ave (nm) | ZP (mV) | Z-Ave (nm) | ZP (mV) | Z-Ave (nm) | ZP (mV) | Z-Ave (nm) | ZP (mV) |
| 1 | 385.20 ± 0.21 | -27.50 ± 0.10 | 391.30 ± 0.22 | -37.80 ± 0.13 | 428.07 ± 0.13 | -34.20 ± 0.10 | 437.20 ± 0.10 | -31.87 ± 0.01 |
| 90 | 495.70 ± 0.33 | -28.80 ± 0.11 | 471.50 ± 0.41 | -39.4 ± 0.12 | 549.63 ± 0.10 | -37.77 ± 0.12 | 479.57 ± 0.12 | -37.63 ± 0.11 |

Table 3
Rheological characterization of the HG_PF-NP formulations after 8 and 90 days of storage at 25 °C.

| Time Days | HG_PF-F1NPs | | HG_PF-F2NPs | | HG_PF-F1NPs-Azone | | HG_PF-F2NPs-Azone | |
|--------------|------------------|-------------------|------------------|-------------------|-------------------|-------------------|-------------------|-------------------|
| | Viscosity (Pa s) | Thixotropy (Pa/s) | Viscosity (Pa s) | Thixotropy (Pa/s) | Viscosity (Pa s) | Thixotropy (Pa/s) | Viscosity (Pa s) | Thixotropy (Pa/s) |
| 8 | 1.64 ± 0.002 | 586.30 | 2.38 ± 0.001 | 1935.03 | 2.70 ± 0.002 | 3562.01 | 2.95 ± 0.002 | 3281.50 |
| 90 | 1.10 ± 0.001 | 542.45 | 0.93 ± 0.002 | 555.10 | 1.99 ± 0.001 | 3290.63 | 2.08 ± 0.002 | 3061.30 |

of the elastic over the viscous behavior ($G' > G''$) for all the HG_PF-NP formulations.

3.3. *In vitro* drug release

An *in vitro* release study of pranopfen from the HG_PF-NP formulations, free drug solution (pranopfen, dissolved in PBS) and commercial eye drops (Oftalar[®], pranopfen 1.0 mg/mL) was performed in Franz diffusion cell. As shown in Fig. 2, the release profile of pranopfen from the free drug solution and the commercial eye drops exhibited faster release than from the HG_PF-NP formulations with or without azone. After 3 h, 100% of the drug was released from the free drug solution or commercial eye drops. Fig. 2 reveals that the HG_PF-NP formulations with or without azone exhibit a sustained release behavior. The accumulative amount of pranopfen released from HG_PF-F1NPs, HG_PF-F2NPs, HG_PF-F1NPs-Azone and HG_PF-F2NPs-Azone after 24 h was 41.99%, 64.35%, 56.75% and 59.14%, respectively. Fig. 2 also shows that the amount released of pranopfen from HG_PF-F1NPs and HG_PF-F1NPs-Azone was slightly smaller than HG_PF-F2NPs and HG_PF-F2NPs-Azone, respectively. These results might be attributed to the fact that during the preparation of the NPs the viscosity increases when there is an increase in the cPVA from 5 mg/mL (PF-F2NPs) to 10 mg/mL (PF-F1NPs). This viscosity increase could result in a more compact polymer matrix leading to slower degradation of the polymer or slower diffusion of the loaded pranopfen from the nanoparticles [40].

In previous studies, we assessed the release profile of pranopfen from the PF-F1NP and PF-F2NP formulations. The results obtained from this study revealed that both formulations showed a sustained release behavior, with an initial burst attributed to the pranopfen adsorbed onto the nanoparticles' surface, followed by a slower release phase while the trapped pranopfen slowly diffuses out of the polymeric matrix into the release medium [20]. However, the pranopfen release rate was faster from the pranopfen-loaded nanoparticles than from the hydrogel formulations with or without azone. All these results suggest that the diffusion velocity of pranopfen from the nanoparticles can be modified due to higher viscosity of the hydrogels respect to the nanoparticle suspensions. Nevertheless, the pranopfen-loaded

nanoparticles or hydrogels with or without azone could offer sustained release of the drug in comparison with the free drug solution or commercial eye drops.

The amount of pranopfen released from the HG_PF-F1NPs, HG_PF-F2NPs, HG_PF-F1NPs-Azone, HG_PF-F2NPs-Azone, commercial eye drops and free drug solution was adjusted to various kinetic models, such as zero-order, first-order, Higuchi, Hyperbola and Korsmeyer–Peppas (Table 4). The AIC was determined for each model. This parameter is an indicator of the model's suitability for a given dataset. The smaller the value of AIC, the better the model adjusts the data.

From the AIC values (Table 4), it can be concluded that the release curves of pranopfen from HG_PF-F1NPs, HG_PF-F2NPs, HG_PF-F2NPs-Azone, commercial eye drops and free drug solution fitted to the hyperbola model very well. The drug release mechanism of the HG_PF-F1NPs-Azone formulation differed respect to the other formulations, which adjusted to the first order model. These models had the smaller AIC value and, therefore, statistically, described best the drug release mechanism. Taking into account the diffusional exponent value (n) that is used to characterize different release mechanisms, n values ≤ 0.5 were obtained in all the investigated HG_PF-NP formulations indicating that the release of pranopfen from the semi-solid formulations occurs by passive diffusion. All these results suggest that the main factors that govern the release of the pranopfen from the HG_PF-NP formulations with or without azone are the amount of PVA present in the formulation. Furthermore, the release rate is influenced by the presence of pranopfen in crystalline form, since the drug in crystalline form should dissolve first before being transported out to the matrix by diffusion. As previously reported, in our study that the intensity of some of the peaks of crystalline pranopfen present in the nanoparticles slightly increased when the concentration of the drug increased from 1.0 mg/mL (PF-F2NPs) to 1.5 mg/mL (PF-F1NPs) by X-ray diffraction technique [20]. Additionally, the drug diffusion out of a hydrogel matrix dependent on mechanical strength degradability, diffusivity, and other physical properties of hydrogel network [41].

3.4. Corneal permeation study

Ex vivo corneal permeation study has been carried out up to 6 h, to compare the permeation profile of pranopfen from the hydrogel formulations with or without azone, commercial eye drops and free drug solution, and the results are shown in Fig. 3. The permeation parameter values are summarized in Table 5.

At the end of the corneal permeation study, the cornea was used to determine the amount of drug retained and the corneal hydration level. These results are exhibited in Table 6.

The corneal permeation parameters of pranopfen calculated from the amounts of permeated across cornea from the hydrogel formulations with or without azone, commercial eye drops and free drug solution in Table 5 were compared by the application of a non-parametric statistical Kruskal–Wallis Z test followed by the Dunn's multiple comparison tests. From the statistical analysis of the K_p parameter obtained from these formulations, statistically significant differences ($p < 0.05$) were found between HG_PF-F1NPs and HG_PF-F2NPs, HG_PF-F1NPs and commercial eye drops,

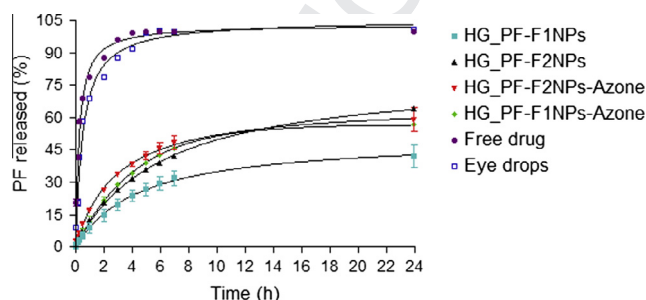


Fig. 2. *In vitro* release profiles of PF from HG_PF-F1NPs, HG_PF-F2NPs, HG_PF-F1NPs-Azone, HG_PF-F2NPs-Azone, commercial eye drops and free drug solution. Mean \pm SD, $n = 3$. (For the interpretation of the references to color in this figure legend, the reader is referred to the web version of this article.)

Table 4

Mean parameter obtained after fitting the release data of HG_PF-F1NPs, HG_PF-F2NPs, HG_PF-F1NPs-Azone, HG_PF-F2NPs-Azone, commercial eye drops and free drug solution to different kinetic models.

| Models | Parameters | HG_PF-F1NPs | HG_PF-F2NPs | HG_PF-F1NPs-Azone | HG_PF-F2NPs-Azone | Eye drops | Free drug |
|------------------|------------|-------------|-------------|-------------------|-------------------|-----------|-----------|
| Zero order | AIC | 75.35 | 80.67 | 86.52 | 88.03 | 110.78 | 109.76 |
| First Order | AIC | 9.40 | 33.32 | -7.46 | 37.01 | 70.48 | 67.21 |
| Higuchi | AIC | 55.12 | 52.86 | 69.11 | 71.01 | 101.97 | 102.63 |
| Hyperbola | | 7.35 | -8.23 | 26.99 | 15.96 | 59.36 | 50.52 |
| Korsmeyer-Peppas | <i>n</i> | 0.50 | 0.50 | 0.50 | 0.50 | 0.38 | 0.28 |
| | AIC | 55.20 | 53.22 | 69.20 | 72.62 | 110.27 | 115.37 |

n, diffusional release exponent; AIC, Akaike information criterion.

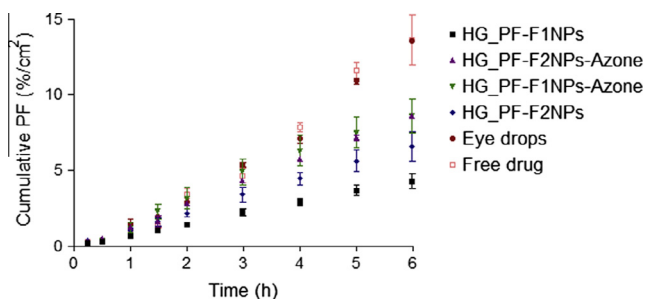


Fig. 3. Ex vivo corneal permeation profile of PF from the HG_PF-F1NPs, HG_PF-F2NPs, HG_PF-F1NPs-Azone, HG_PF-F2NPs-Azone formulations, commercial eye drops and free drug solution after 6 h. Mean \pm SD, *n* = 6. (For the interpretation of the references to color in this figure legend, the reader is referred to the web version of this article.)

HG_PF-F1NPs-Azone and HG_PF-F2NPs, HG_PF-F1NPs-Azone and commercial eye drops. The HG_PF-F1NPs and HG_PF-F2NPs show the lowest and highest K_p value, respectively. Statistically significant differences ($p < 0.05$) were found between HG_PF-F1NPs and HG_PF-F2NPs, HG_PF-F1NPs and commercial eye drops, HG_PF-F1NPs and free drug, HG_PF-F2NPs-Azone and free drug, HG_PF-

F1NPs-Azone and commercial eye drops, HG_PF-F1NPs-Azone and free drug for the P_1 parameter. As shown in Table 5 the free drug solution and HG_PF-F1NPs formulation exhibited the highest and lowest P_1 value, respectively. The statistical analysis of the P_2 and T_L parameters in Table 5 revealed a significant difference ($p < 0.05$) between HG_PF-F1NPs and commercial eye drops, HG_PF-F1NPs and free drug, HG_PF-F2NPs-Azone and free drug, HG_PF-F1NPs-Azone and commercial eye drops, HG_PF-F1NPs-Azone and free drug. The HG_PF-F1NP formulation exhibits the highest P_2 value and the lowest P_1 value, thus this formulation shows the lowest K_p value, since K_p depends directly of P_1 and P_2 . The K_p values obtained for the HG_PF-F2NP formulation, commercial eye drops and free drug solution are directly related to the P_1 parameter. Otherwise, the P_2 values exhibited for the HG_PF-F1NPs-Azone and HG_PF-F2NPs-Azone suggest that the diffusion coefficient of a drug is influenced by the presence of azone in the formulation. The T_L values obtained in Table 5 for the HG_PF-NPs with or without azone are lower than those obtained for the commercial eye drops and free drug solution. Therefore, these formulations reach faster the steady state equilibrium than the commercial eye drops and free drug solution.

The Q_p and Q_R values obtained for the commercial eye drops and free drug solution are greater than those obtained for the hydrogel

Table 5

Corneal permeation parameters of PF from HG_PF-NP formulations, commercial eye drops and free drug solution after 6 h.

| Samples | $K_p \times 10^2$ (cm/h) | $P_1 \times 10^1$ (cm) | $P_2 \times 10^1$ (h ⁻¹) | $T_L \times 10^1$ (h) |
|-------------------|---------------------------------|-----------------------------------|--------------------------------------|-----------------------------------|
| HG_PF-F1NPs | 1.50 (1.32–1.72) ^{b,e} | 0.05 (0.04–0.05) ^{b,e,f} | 32.64 (24.61–40.67) ^{e,f} | 0.54 (0.41–0.68) ^{e,f} |
| HG_PF-F2NPs | 5.56 (4.10–7.03) ^{a,c} | 0.61 (0.53–0.69) ^a | 8.98 (7.80–10.16) | 1.90 (1.64–2.14) |
| HG_PF-F1NPs-Azone | 2.68 (2.62–2.72) ^{b,e} | 0.11 (0.08–0.14) ^{e,f} | 25.87 (18.09–33.66) ^{e,f} | 0.71 (0.50–0.92) ^{e,f} |
| HG_PF-F2NPs-Azone | 3.26 (3.27–3.29) | 0.20 (0.16–0.24) ^f | 16.93 (13.39–20.47) ^f | 1.03 (0.81–1.25) ^f |
| Eye drops | 3.46 (3.42–3.62) ^{a,c} | 0.89 (0.77–0.91) ^{a,c} | 3.98 (3.87–4.47) ^{a,c} | 4.19 (3.73–4.31) ^{a,c} |
| Free drug | 3.32 (3.28–3.56) | 1.00 (0.93–1.07) ^{a,d,c} | 3.30 (3.06–3.84) ^{a,d,c} | 5.00 (4.34–5.45) ^{a,d,c} |

Results are reported as median value (minimum–maximum range) *n* = 6.

- ^a Differences with HG_PF-F1NPs.
- ^b Differences with HG_PF-F2NPs.
- ^c Differences with HG_PF-F1NPs-Azone.
- ^d Differences with HG_PF-F2NPs-Azone.
- ^e Commercial eye drops.
- ^f Free drug solution.

Table 6

Amounts of PF permeated (Q_p) and retained (Q_R) across cornea and corneal hydration level (HL) from the HG_PF-NP formulations, commercial eye drops and free drug solution after 6 h.

| Samples | Q_p (%/cm ²) | Q_R (%/cm ² g) | HL (%) |
|-------------------|----------------------------|-----------------------------|---------------------|
| HG_PF-F1NPs | 4.28 (3.6–4.93) | 18.23 (15.21–19.61) | 79.87 (76.18–80.03) |
| HG_PF-F2NPs | 6.58 (5.35–7.08) | 16.32 (16.17–16.64) | 77.56 (77.25–79.80) |
| HG_PF-F1NPs-Azone | 8.57 (7.20–9.59) | 24.56 (23.38–25.57) | 76.98 (76.57–78.87) |
| HG_PF-F2NPs-Azone | 6.61 (8.51–8.17) | 20.71 (16.64–24.60) | 78.19 (77.87–79.67) |
| Eye drops | 13.53 (11.12–13.57) | 52.55 (51.23–53.62) | 77.44 (78.23–79.87) |
| Free drug | 13.62 (11.58–15.46) | 50.41 (49.91–50.19) | 78.12 (76.67–79.98) |

Results are reported as median value and minimum – maximum range values (Q_p , *n* = 6; Q_R , *n* = 3; HL, *n* = 3).

formulations with or without azone (Table 6). Nevertheless, the free drug solution is inherently irritating to the eye and additionally, pranopfen is unstable in aqueous solution [42]. Otherwise, the increased in the corneal permeation of pranopfen showed for the commercial eye drops can be explained due to this conventional dosage form has a combination of benzalkonium chloride (BAK) and edetate disodium (EDTA). The BAK produces an increase of the amount of drug permeating the cornea by disruption of the corneal epithelium. Additionally, it can also emulsify the corneal epithelium, leading to increased partitioning of the drug [43]. Moreover, EDTA also increases the corneal permeability of different drugs, by removing the extracellular calcium ions increasing tight junction permeability [22,44,45].

Table 6 also shows that the Q_p and Q_R values of pranopfen in the cornea from the HG_PF-F1NPs-Azone and HG_PF-F2NPs-Azone formulations are greater than those obtained from HG_PF-F1NPs and HG_PF-F2NPs, respectively. The results suggest that the inclusion of azone into HG formulation leads to the increase in the amount of drug permeated and retained. Azone is one of the most widely studied penetration enhancers of hydrophilic and lipophilic drugs, which can be used as a safe and effective penetration enhancer for human. Azone as a penetration enhancer is most effective at low percentages; values ranging from 1% to 3% had been reported in the literature. Although azone has been used for over 25 years, several researchers continue to investigate its mechanism of action. The mechanism of azone may be related with modifications in the epithelial cell junctions and enhanced the influx of water and the transcorneal penetration of hydrophilic drugs but delayed the apparent drug permeation of lipophilic drugs through the cornea [22,23]. Regarding the corneal hydration analysis, the healthy cornea has a hydration level of 76–80% [46]. According to the results obtained in Table 6 for the HG_PF-NP formulations with or without azone, commercial eye drops and free drug solution, it can be concluded that during the assay the cornea was no damage.

3.5. In vitro ocular tolerance

The studies using the HET-CAM are based on the direct application of the sample onto the chorioallantoic membrane and the observation of reactions, such as hemorrhage, intravasal coagulation or lysis of blood vessels [47]. The results of the HET-CAM test revealed optimal ocular tolerance of the HG_PF-NPs with or without azone since no irritation reactions were detected within 5 min of the assay (score 0).

3.6. In vivo ocular tolerance

Durand-Cavagna et al. evaluated in rabbits the ocular irritation potential of 1% or 2% azone incorporated in ophthalmic vehicles, such as poloxamer 188, hydroxyl-ethylcellulose, benzalkonium chloride and phosphate buffer. Signs of ocular irritation were detected. However, the reported results were inconclusive since irritation could not be attributed to the presence of azone or benzalkonium chloride [48]. In the present work, the irritancy of the optimized HG_PF-NP formulations with or without azone was evaluated in New Zealand white rabbits. The results of Draize test showed good ocular tolerance of HG_PF-NPs with a 0% or 1% azone. No signs of ocular irritancy were detected. These results are in accordance with those obtained by HET-CAM test.

3.7. In vivo anti-inflammatory efficacy

Fig. 4 shows the anti-inflammatory efficacy effect of different formulations containing pranopfen in the ocular edema induced by instillation of SA.

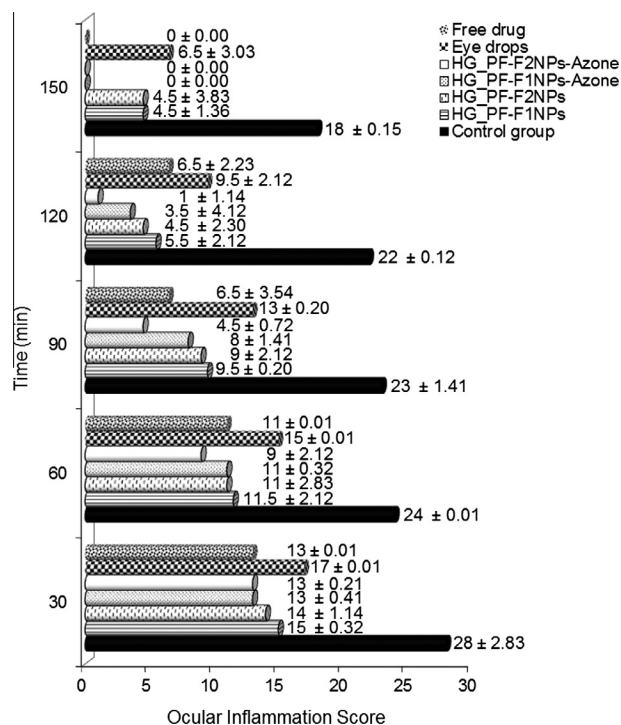


Fig. 4. Anti-inflammatory activity of PF from the HG_PF-F1NPs, HG_PF-F2NPs, HG_PF-F1NPs-Azone, HG_PF-F2NPs-Azone formulations, commercial eye drops and free drug solution. Mean ± SD. n = 6.

Although the commercial eye drops and free drug solution show the highest Q_R values of pranopfen in the cornea, the anti-inflammatory efficacy values obtained for the commercial eye drops are lower compared to the other tested formulations (Fig. 4). Until 120 min, the free drug solution exhibits slower anti-inflammatory activity than the HG_PF-NP formulation with or with azone. The results obtained for the commercial eye drops and free drug solution could be explained by the fact that these formulations show T_L values greater than those obtained for the HG_PF-NPs with or without azone. Thus, the commercial eye drops and free drug solution reach slower steady state equilibrium than the HG_PF-NPs, therefore show slower anti-inflammatory activity than the other tested formulation. Fig. 4 also shows that the HG_PF-F1NPs-Azone and HG_PF-F2NPs-Azone formulations significantly reduced the ocular edema, compared to the HG_PF-F1NP and HG_PF-F2NP formulations, respectively. According to the results obtained in this study, the inclusion of azone into the HG_PF-NP formulations leads to the increase of the anti-inflammatory efficacy of pranopfen in the cornea. The anti-inflammatory efficacy values exhibited for the HG_PF-F1NPs-Azone and HG_PF-F2NPs-Azone formulations are correlated directly with the amount of drug retained in the cornea. Therefore, the ocular application of the HG_PF-F1NPs-Azone or HG_PF-F2NPs-Azone formulations could more effective in the treatment of ocular edema that the HG_PF-F1NP or HG_PF-F2NP formulations.

4. Conclusions

The optimized PF-F1NP and PF-F2NP suspensions were successfully dispersed into blank hydrogels or hydrogels containing 1% azone. The hydrogel formulations showed a rheological behavior and physicochemical properties suitable for ocular pranopfen delivery. The HG_PF-NPs with or without azone exhibited sustained release behavior with a slower release of pranopfen. According to the results obtained from the corneal permeation

and anti-inflammatory efficacy studies, the commercial eye drops and free drug solution showed the highest Q_R values of pranoprofen in the cornea. However, both formulations cannot be considered optimal in the treatment of ocular diseases due to the free drug solution is inherently irritating to the eye and additionally, pranoprofen is unstable in aqueous solution. Besides, following the instillation of commercial eye drops, the most of the drugs is removed, by ear dilution and tear turn over from the surface of the eye due to the low viscosity of these conventional dosage forms. The HG_PF-F1NPs-Azone and HG_PF-F2NPs-Azone formulations significantly reduced the ocular edema, compared with other tested formulations. These results indicate that the inclusion of azone into the HG_PF-NP formulations leads to the increase of the anti-inflammatory efficacy effect of pranoprofen in the cornea. Therefore, the ocular application of these formulations could be more effective in the treatment of ocular edema.

The HG_PF-NPs with 0% or 1% azone showed an optimal ocular tolerance by the *in vitro* and *in vivo* ocular irritation test. All these results suggest that the ocular administration of the HG_PF-F1NPs-Azone or HG_PF-F2NPs-Azone formulations could be an effective and appropriate system for ophthalmic administration of pranoprofen, improving the biopharmaceutical profile of this drug, thus enhancing the local anti-inflammatory and analgesic effect of this drug and, consequently, improving the patient's compliance. However, the formulations for ocular applications based on carbomer hydrogels must be preserved in order to avoid the growth of microorganisms, but unfortunately the action of the ophthalmic preservatives is non-specific and these can cause toxicity or damage to the ocular structure. In order to ensure the conservation of the HG_PF-NP formulation, additional studies related to sterilization by autoclave or gamma irradiation would be required.

Conflict of interest

The authors declare that they have no conflict of interest.

Acknowledgments

G. Abrego wishes to acknowledge, the Spanish Ministry of Foreign Affairs and Cooperation and the Spanish Agency for International Development Cooperation (MAEC-AECID) for a research scholarship. The authors would also like to acknowledge the financial support of the Spanish Ministry of Science and Innovation (Grant MAT2011-26994), Portuguese Science and Technology Foundation (FCT), and European funds (FEDER/COMPETE) under the reference PTDC/SAU-FAR/113100/2009.

Appendix A. Supplementary data

Supplementary data associated with this article can be found, in the online version, at <http://dx.doi.org/10.1016/j.ejpb.2015.01.026>.

References

- [1] I. Akyol-Salman, D. Leçe-Sertöz, O. Baykal, Topical pranoprofen 0.1% is as effective anti-inflammatory and analgesic agent as diclofenac sodium 0.1% after strabismus surgery, *J. Ocul. Pharmacol. Ther.* 23 (2007) 280–283.
- [2] M. Sawa, K. Masuda, M. Nakashima, Anti-inflammatory effect of diclofenac sodium eye drops on cataract surgery. Double masked study with pranoprofen eye drops, *IOL RS* 13 (1999) 193–200.
- [3] A.Z. McCollgin, J.S. Heier, Control of intraocular inflammation associated with cataract surgery, *Curr. Opin. Ophthalmol.* 11 (2000) 3–6.
- [4] X. Liu, S. Wang, A.A. Kao, Q. Long, The effect of topical pranoprofen 0.1% on the clinical evaluation and conjunctival HLA-DR expression in dry eyes, *Cornea* 31 (2012) 1235–1239.
- [5] R. Notivol, M. Martinez, M. Bergamini, Treatment of chronic nonbacterial conjunctivitis with a cyclo-oxygenase inhibitor or a corticosteroid. Pranoprofen Study Group, *Am. J. Ophthalmol.* 117 (1994) 651–656.

- [6] M. Narashino, H. Ichikawa, S. Narita, A.S. Yotsukaido, Sustained-Release Pranoprofen Preparation, US00522506A, 1993.
- [7] K. Koba, H. Otsu, Y. Koba, Y. Kakogawa, Method for Stabilizing Pranoprofen and Stable Liquid Preparation of Pranoprofen, United States Patent. US005856345A, 1999.
- [8] J. Araújo, E. Gonzalez, M.A. Egea, M.L. Garcia, E.B. Souto, Nanomedicines for ocular NSAIDs: safety on drug delivery, *Nanomedicine: Nanotechnol. Biol. Med.* 5 (2009) 394–401.
- [9] L.S. Nair, C.T. Laurencin, Biodegradable polymers as biomaterials, *Prog. Polym. Sci.* 32 (2007) 762–798.
- [10] A. Sabzevari, K. Adibkia, H. Hashemi, A. Hedayatfar, N. Mohsenzadeh, F. Ataybi, M.H. Ghahremani, R. Dinarvand, Polymeric triamcinolone acetonide nanoparticles as a new alternative in the treatment of uveitis: *in vitro* and *in vivo* studies, *Eur. J. Pharm. Biopharm.* 84 (2013) 63–67.
- [11] E. Vega, M.A. Egea, M.L. Garduño-Ramírez, M.L. García, E. Sánchez, M. Espina, A.C. Calpena, Flurbiprofen PLGA-PEG nanospheres: role of hydroxy- β -cyclodextrin on *ex vivo* human skin permeation and *in vivo* topical anti-inflammatory efficacy, *Colloids Surf. B. Biointerfaces* 110 (2013) 339–346.
- [12] S.P. Ayalassomayajula, U.B. Kompella, Subconjunctivally administered celecoxib-PLGA microparticles sustain retinal drug levels and alleviate diabetes-induced oxidative stress in a rat model, *Eur. J. Pharmacol.* 511 (2005) 191–198.
- [13] T. Gratieri, G.M. Gelfuso, E.M. Rocha, V.H. Sarmento, O. de Freitas, R.F.V. Lopez, A poloxamer/chitosan *in situ* forming gel with prolonged retention time for ocular delivery, *Eur. J. Pharm. Biopharm.* 75 (2010) 186–193.
- [14] A. Lauterbach, C.C. Müller-Goymann, Comparison of rheological properties, follicular penetration, drug release, and permeation behavior of a novel topical drug delivery system and a conventional cream, *Eur. J. Pharm. Biopharm.*, doi: 10.1016/j.ejpb.2014.10.001.
- [15] A. Zoppi, Y.G. Linck, G.a. Monti, D.B. Genovese, A.F. Jimenez Kairuz, R.H. Manzo, M.R. Longhi, Studies of pilocarpine:carbomer intermolecular interactions, *Int. J. Pharm.* 427 (2012) 252–259.
- [16] B. Buchan, G. Kay, A. Heneghan, K.H. Matthews, D. Cairns, Gel formulations for treatment of the ophthalmic complications in cystinosis, *Int. J. Pharm.* 392 (2010) 192–197.
- [17] P. Batheja, L. Sheihet, J. Kohn, A.J. Singer, B. Michniak-Kohn, Topical drug delivery by a polymeric nanosphere gel: Formulation optimization and *in vitro* and *in vivo* skin distribution studies, *J. Control. Release.* 149 (2011) 159–167.
- [18] F.E. Amara, M.E. Meleis, M.A. Seif, E.Y. Moursy, Study of the metabolic effect and histopathological nasal mucosal changes after prolonged intranasal insulin administration, *J. Diabetol.* 1 (2011) 1–10.
- [19] H. Fessi, F. Puisieux, J.P. Devissaguet, N. Ammoury, S. Benita, Nanocapsule formation by interfacial polymer deposition following solvent displacement, *Int. J. Pharm.* 55 (1989) R1–R4.
- [20] G. Abrego, H.L. Alvarado, M.A. Egea, E. Gonzalez-Mira, A.C. Calpena, M.L. Garcia, Design of nanosuspensions and freeze-dried PLGA nanoparticles as a novel approach for ophthalmic delivery of pranoprofen, *J. Pharm. Sci.* 103 (2014) 3153–3164.
- [21] J.R. Robinson, Ocular drug delivery mechanism(s) of corneal drug transport and mucoadhesive delivery systems, *STP Pharma* 5 (1989) 839–846.
- [22] I.P. Kaur, R. Smitha, Penetration enhancers and ocular bioadhesives: two new avenues for ophthalmic drug delivery, *Drug Dev. Ind. Pharm.* 28 (2002) 353–369.
- [23] A.C. Williams, B.W. Barry, Penetration enhancers, *Adv. Drug Deliv. Rev.* 64 (2012) 128–137.
- [24] F. Lallemand, O. Felt-Baeyens, K. Besseghir, F. Behar-Cohen, R. Gurny, Cyclosporine A delivery to the eye: a pharmaceutical challenge, *Eur. J. Pharm. Biopharm.* 56 (2003) 307–318.
- [25] I.M. Ismail, C.C. Chen, J.B. Richman, J.S. Andersen, D.D. Tang-Liu, Comparison of azone and hexamethylene lauramide in toxicologic effects and penetration enhancement of cimetidine in rabbit eyes, *Pharm. Res.* 9 (1992) 817–818.
- [26] T.J. Franz, Percutaneous absorption. On the relevance of *in vitro* data, *J. Invest. Dermatol.* 64 (1975) 190–195.
- [27] P. Costa, J.M. Sousa, Modeling and comparison of dissolution profiles, *Eur. J. Pharm.* 13 (2001) (2001) 123–133.
- [28] K. Yamaoka, T. Nakagawa, T. Uno, Application of Akaike's information criterion (AIC) in the evaluation of linear pharmacokinetic equations, *J. Pharmacokinet. Biopharm.* 6 (1978) 165–175.
- [29] N.P. Luepke, Heng's egg chorioallantoic membrane test for irritation potential, *Food Chem.* 23 (1985) 287–291.
- [30] M. Warren, K. Atkinson, S. Steer, Invitox-protocol: the Ergatt/Frame data bank of *in vitro* techniques in toxicology, *Heft egg test.* Nr 15 (4) (1990) 707–710.
- [31] Journal Officiel de la République Française. Méthode Officiel d'évaluation du potentiel irritant par application sur la membrane chorioallantoïdienne de l'oeuf de poule. Annexe IV. (1996) 1937–1938.
- [32] J. Draize, G. Woodard, H. Calvery, Methods for the study of irritation and toxicity of substances applied topically to the skin and mucous membranes, *J. Pharmacol. Exp. Ther.* 82 (1944) 377–390.
- [33] J.H. Kay, J.K. Calandra, Interpretation of eye irritation test, *J. Soc. Cosmet. Chem.* 13 (1962) 281–289.
- [34] S. Spampinato, A. Marino, C. Bucolo, M. Canossa, T. Bachetti, S. Mangiafico, Effects of sodium naproxen eye drops on rabbit ocular inflammation induced by sodium arachidonate, *J. Ocul. Pharmacol.* 7 (1991) 125–133.
- [35] E. Gonzalez-Mira, S. Nikolić, A.C. Calpena, M.A. Egea, E.B. Souto, M.L. Garcia, Improved and safe transcorneal delivery of flurbiprofen by NLC and NLC-based hydrogels, *J. Pharm. Sci.* 101 (2012) 707–725.

- 878 [36] A. Zimmer, J. Kreuter, Microspheres and nanoparticles used in ocular delivery 893
879 systems, *Ocul. Drug Deliv. Rev.* 168 (1995) 61–73. 894
- 880 [37] X. Song, Y. Zhao, S. Hou, F. Xu, R. Zhao, J. He, Z. Cai, Y. Li, Q. Chen, Dual agents 895
881 loaded PLGA nanoparticles: systematic study of particle size and drug 896
882 entrapment efficiency, *Eur. J. Pharm. Biopharm.* 69 (2008) 445–453. 897
- 883 [38] F. Han, R. Yin, X. Che, J. Yuan, Y. Cui, H. Yin, S. Li, Nanostructured lipid carriers 898
884 (NLC) based topical gel of flurbiprofen: design, characterization and *in vivo* 899
885 evaluation, *Int. J. Pharm.* 439 (2012) 349–357. 900
- 886 [39] Malvern Instruments. 10 Ways to Control Rheology by Changing Particles 901
887 Properties. INFORM Series of White Papers, 2009. 902
- 888 [40] S.K. Sahoo, J. Panyam, S. Prabha, V. Labhasetwar, Residual polyvinyl alcohol 903
889 associated with poly (d, l-lactide-co-glycolide) nanoparticles affects their 904
890 physical properties and cellular uptake, *J. Control Release* 82 (2002) 105–114. 905
- 891 [41] M. Hamidi, A. Azadi, P. Rafei, Hydrogel nanoparticles in drug delivery, *Adv.* 906
892 *Drug Deliv. Rev.* 60 (2008) 1638–1649. 907
- [42] M. Ahuja, A.S. Dhake, S.K. Sharma, D.K. Majumdar, Topical ocular delivery of 893
NSAIDs, *AAPS J.* 10 (2008) 229–241. 894
- [43] M.S. Rathore, D.K. Majumdar, Effect of formulation factors on *in vitro* 895
transcorneal permeation of gatifloxacin from aqueous drops, *AAPS* 896
PharmSciTech. 7 (2006) E1–E6. 897
- [44] K. Järvinen, T. Järvinen, A. Urtti, Ocular absorption following topical delivery, 898
Adv. Drug Deliv. Rev. 16 (1995) 3–19. 899
- [45] P. Furrer, J.M. Mayer, R. Gurny, Ocular tolerance of preservatives and 900
alternatives, *Eur. J. Pharm. Biopharm.* 53 (2002) 263–280. 901
- [46] R.D. Schoenwald, H.S. Huang, Corneal penetration behavior of beta-blocking 902
agents I: physiochemical factors, *J. Pharm. Sci.* 72 (1983) 1266–1272. 903
- [47] J. Tavaszi, P. Budai, The use of HET-CAM test in detecting the ocular irritation, 904
Commun. Agric. Appl. Biol. Sci. 72 (2007) 137–141. 905
- [48] G. Durand-Cavagna, P. Duprat, S. Molon-Noblot, P. Delort, A. Rozier, Corneal 906
endothelial changes with Azone, a penetration enhancer, *Lens Eye Toxic. Res.* 6 907
(1989) 109–117. 908
909
910

UNCORRECTED PROOF